JOURNAL OF ADVANCED TRANSPORTATION
J. Adv. Transp. 2013; **47**:635–649
Published online 30 December 2011 in Wiley Online Library (wileyonlinelibrary.com). DOI: 10.1002/atr.186

Visco-elastic traffic flow model

Zuojin Zhu[1]* and Chun Yang[2]

[1]*Department of Thermal Science and Energy Engineering, University of Science and Technology of China, Hefei, Anhui 230026, China*
[2]*School of Mechanical and Aerospace Engineering, Nanyang Technological University, Singapore, 639798*

SUMMARY

To increase our understanding of the operations of traffic system, a visco-elastic traffic model was proposed in analogy of non-Newtonian fluid mechanics. The traffic model is based on mass and momentum conservations, and includes a constitutive relation similar to that of linear visco-elastic fluids. The further inclusion of the elastic effect allows us to describe a high-order traffic model more comprehensively because the use of relaxation time indicates that vehicle drivers adjust their time headway in a reasonable and safe range. The self-organizing behaviour is described by introducing the effects of pressure and visco-elasticity from the point of view in fluid mechanics. Both the viscosity and elasticity can be determined by using the relaxation time and the traffic sound speed. The sound speed can be approximately represented by the road operational parameters including the free-flow speed, the jam density, and the density of saturation if the jam pressure in traffic flows is identical to the total pressure at the flow saturation point. A linear stability analysis showed that the traffic flow should be absolutely unstable for disturbances with short spatial wavelengths. There are two critical points of regime transition in traffic flows. The first point happens at the density of saturation, and the second point occurs at a density relating on the sound speed and the fundamental diagram of traffic flows. By using a triangular form flow–density relation, a numerical test based on the new model is carried out for congested traffic flows on a loop road without ramp effect. The numerical results are discussed and compared with the result of theoretical analysis and observation data of traffic flows.

KEY WORDS: visco-elastic traffic model; congested traffic flows; traffic relaxation time; traffic sound speed

1. INTRODUCTION

Traffic flow has been extensively studied because of its great importance to our modern society. Numerous traffic flow models have been developed. The well-known (Lighthill Whitham Richards) LWR model [1,2] merely based on vehicular mass conservation is probably the simplest one and is capable of capturing the important features of traffic flows on highways, such as the traffic shock waves propagating in steeper slope of wave front. However, the LWR model cannot more satisfactorily predict the stop and moving waves that might be caused by red lights or traffic accidents. Nevertheless, the development of the extended LWR models has been reported to be capable of predicting the traffic hysteresis [3], observing the evolution of density waves [4] as well as explaining the critical transition in bottleneck affected traffic [5].

The traffic flow models additionally concerned with vehicular momentum conservation are usually termed as high-order models, among which we should mention the historical works based on the Euler equation [6] and the gas-kinetic analogy [7]. The high-order models are successful in elucidating the stop and moving phenomena in traffic and predicting traffic wave propagations, even though there is a critic comment [8] that the high-order models are ineffective, which hinders not only the application [9–11] but also the further development of high-order traffic flow models [12–16].

*Correspondence to: Zuojin Zhu, Department of Thermal Science and Energy Engineering, University of Science and Technology of China, Hefei, Anhui 230026, China. E-mail: zuojin@ustc.edu.cn

There are also other kinds of traffic models based on the artificially assigned rules and computer-game operations. These models are distinguished by the rules and are usually called as cellular automaton [17–19], and the aim of these models is to find the state relation under traffic equilibrium by a statistical decoupling. Traffic systems have been reported to have a surprisingly rich spectrum of spatio-temporal pattern formation phenomena. Nagatani [20] has discussed the main models of traffic including the car-following models, the cellular automaton models, the gas-kinetic models and the fluid-dynamical models. By applying and extending methods from statistical physics and nonlinear dynamics to self-driven many-particle systems, Helbing [21] had explained some questions concerned with vehicle traffic.

Despite that some existing high-order models utilize traffic relaxation time to denote the external force on vehicles in the momentum equation, there is little information associated with the elastic behaviour of vehicular clusters. Vehicle drivers intend to adjust their time headway to a value close to the reciprocal of the traffic capacity. The vehicle driving behaviour was mentioned by Del Castillo [22], who developed a random-motion model to consider the propagation of speed perturbations in congested traffic flow. He remarked that even if changes like ramps and tunnels are not present, speed variation is always present because of the random and non-homogeneous nature of driver behaviour. Traffic speed variations in random form can also be found in the online material [23].

In this paper, with the principles of fluid mechanics, we develop a visco-elastic traffic model (VEM), in which the viscosity and elasticity of traffic can be determined by using the traffic sound speed and the traffic relaxation time. There are two noticeable features of considering the elasticity in modelling traffic flows: the viscosity in traffic flows has some relation to driver's memory, which can be seen in the previous work [24]; the relaxation time used to denote the external force implies the traffic flows involved with an elastic effect. In the proposed model, the relaxation time is assumed to be the travel time of an infinitesimal disturbance through a given distance, such as the spatial step used in numerical simulation of traffic flows. The sound speed can be represented approximately by the free-flow speed, the jam density and the density at traffic saturation if the jam pressure in traffic flows is identical to the total pressure at the saturation point. A linear stability analysis is carried out to evaluate a criterion for traffic flow, which indicates that the visco-elastic traffic flows are absolutely unstable for larger wave numbers. There are two critical points: the first point corresponds to the flow transition from a free-flow stable regime to an oscillating unstable regime; the second point is related to the flow transition from an oscillating unstable regime to another homogeneously stable regime.

Numerical test is carried out using the proposed new model. The simulation results suggest that the second critical point is well consistent with analytically predicted value. When the sound speed in a traffic jam is about 26.11% of the free-flow speed, the critical speed is found to be 15 km/hour, corresponding to a mean spatial headway of about 6 m with the average vehicle length to be set as 5.8 m.

2. VISCO-ELASTIC MODEL

When the instantaneous traffic flow rate (q) is not equal to the flow rate under a traffic equilibrium state (q_e), it is a function of instantaneous density of traffic flow; the vehicle drivers have a tendency of adjusting the speed so that the time headway can approach $1/q_e$. The self-organization phenomenon in traffic flows has been taken into account by introducing the traffic viscosity and pressure in high-order models [25,26]. Because high-order models utilize the traffic relaxation time to represent the external force on vehicles, it seems reasonable to further include the elastic effect on traffic flows because relaxation and elastic processes are inherently related from the view of mechanics. Both the theory of micro-rheology and the experiments on the shear stress of macromolecule polymers have indicated that the sum of relaxation spectra can be represented by a memory function [27]. Furthermore, the instantaneous traffic flow rate does fluctuate near the equilibrium flow rate in reality, which is similar to an elastic process.

It is noted that, in the model introduced later, only the interaction between the lead and follower vehicles is considered. The interaction of vehicles between different lanes occurring in the situations of taking over and lane exchange is not included. As a result, the traffic flow rate and density can be considered as one-dimensional variables.

DOI: 10.1002/atr

Traffic flow rate variation is commonly encountered in congested traffic flows in which the density is larger than the density of saturation as illustrated by ρ_c in Figure 1. The traffic flow rate arrives at the road capacity $q_e(\rho_c)$ at the density of saturation. Therefore, in congested traffic situations, the interaction of vehicles becomes more significant. As a result of density disturbance propagation, the congested traffic flows can occur at a synchronized flow regime in which the flow rate is oscillating or at a jam existing regime [28], whereas highly dense traffic flows are homogeneous and stable [29]. Hence, there should exist a critical point at which a regime transition of congested traffic flow occurs. The theoretical reason can be found in the present model, whose derivation process is presented in this section.

For a linear visco-elastic fluid flow, the shear stress can be expressed as

$$\mathbf{T}_s = \int_0^\infty f(s)\mathbf{H}(s)ds \tag{1}$$

here, f(s) is the memory function. With the experimental observation of the relaxation of shear stress of macromolecule polymer and the theory of micro-rheology [30], we can write the memory function f(s) in the following form

$$f(s) = G\sum_1^N \frac{1}{\tau_j}\exp\left(-s/\tau_j\right) \tag{2}$$

Here, G is the modulus of fluid elasticity, and τ_j is the relaxation time with the jth order.

For simplicity, we make the three following assumptions: (i) the effect of ramp flow resulted from the interaction between the mainline traffic stream and the external environment can be neglected; (ii) the road capacity is insensitive to the vehicle drivers; and (iii) the traffic flow can be seen as one-dimensional flow of linear visco-elastic fluids. The main reason that supports the third assumption is that the relaxation time connecting the elastic and viscous properties of fluids has already been applied in most of the high-order models to represent the driven force of vehicles. Vehicle motion for the drivers' concerns of driving safety has memory behaviour. Therefore, to describe this traffic performance, the use of a memory function is appropriate.

With these assumptions, we start from the constitutive equation of a general linear visco-elastic fluid flow

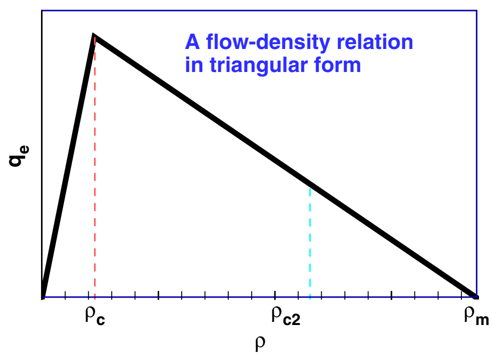

Figure 1. The modelled traffic flow–density relation in triangular form. Note that the density of saturation (ρ_c) is the first critical density, at which there is a flow transition between the free-flow regime and the unstable regime. On the other hand, ρ_{c2} is the second critical density, at which the flow transition between the unstable and homogeneous stable regimes occurs.

DOI: 10.1002/atr

$$\mathbf{T} = -p\mathbf{I} + G\sum_{1}^{N}\int_{0}^{\infty}\frac{1}{\tau_j}\exp\left(-s/\tau_j\right)\mathbf{H}(s)ds \tag{3}$$

where $T = -pI + T_s$ and p are respectively the stress tensor and the traffic pressure, and $\mathbf{I}$ is the unit matrix. $\mathbf{H}(s)$ is the Finger deformation tensor, which can be expressed as $\left(\mathbf{C}^{-1} - \mathbf{I}\right)$,where $\mathbf{C}^{-1}$ is the Finger tensor charactering the scale of the cross-sectional area of a fluid element, and $\mathbf{C}$ is the right Cauchy–Green tensor representing the length scale of a fluid element. For the maximum relaxation order denoted by N, the Finger deformation tensor is given by $\mathbf{H}(s) = \sum_{k=1}^{N}(-1)^{k+1}\frac{s^k}{k!}\mathbf{B}_k$, where $\mathbf{B}_k$ is the White–Metzner tensor, which is defined as $\left[d^k\mathbf{C}^{-1}/dt^k\right]_{t=s}$, and s is the elapsed time period [27].

In the analogy to the unsteady traffic flows, by using the second-order approximation in the case of N=2 and the integration formula $\int_0^{\infty} s^k \exp(-as)ds = k!/a^{k+1}$ merely valid for the positive integer k and the positive real number a, the traffic flow stress can be expressed as follows:

$$T = -p + G(\tau_1 + \tau_2)B_1 - G\left(\tau_1^2 + \tau_2^2\right)B_2 \tag{4}$$

If the traffic speed is defined by u, as shown in APPENDIX A, we have $B_1 = 2u_x$ and

$$B_2 = B_{1t} + uB_{1x} - B_1^2 \tag{5}$$

Because τ_j can be approximated by τ_1/j^2, the total relaxation time can be approximately expressed as $\tau = \tau_1 + \tau_2$. This means that $\tau_1 = 0.8\tau$, and $\tau_2 = 0.2\tau$. Generally, the fluid elasticity is given by $\sigma = 2G\left(\tau_1^2 + \tau_2^2\right)/\rho$. Noting that dynamic viscosity is $\mu = \rho v = 2G\tau$, we can express elasticity as $\sigma = v\left(\tau_1^2 + \tau_2^2\right)/\tau$. This is equivalent to

$$\sigma = v(\tau - 2\tau_1\tau_2/\tau) = 0.68v\tau \tag{6}$$

According to the existing high-order traffic flow models, the general form of the forces acting on vehicular clusters can be formulated by

$$F = -(q - q_e)/\tau + T_x \tag{7}$$

where q_e is the traffic flow rate under the equilibrium traffic state, and T_x is the relevant surface force related to the traffic stress. For the convenience of further analysis, as an example, we use a flow rate that depends on traffic density piecewise linearly (also, in the triangular form as shown in Figure 1)

$$q_e = \begin{cases} v_f\rho, \text{for}\rho \leq \rho_c \\ v_f\rho_c(\rho_m - \rho)/(\rho_m - \rho_c), \text{for}\rho > \rho_c \end{cases} \tag{8}$$

and a traffic pressure

$$p = c_0^2\rho \tag{9}$$

where v_f is the free-flow speed, ρ_m is the jam density, c_0^2 is the anticipation coefficient, and the subscript 'e' represents the relevant variables taken under the equilibrium traffic state. It is necessary to note that the flow–density relation and pressure can also be expressed in other forms, whereas the form availability is explicitly dependent on the traffic operation condition. The equilibrium state mentioned earlier refers to the designed state of traffic road, under which the traffic flow and density satisfy the state

DOI: 10.1002/atr

equation (8). As well known in the society of transportation research, c_0 is the traffic sound speed. It represents how fast the vehicle drivers response to a small speed disturbance. It is expected that the traffic sound speed is close to a constant because it can be approximately denoted by the ratio of the spatial headway to the drivers' reaction time, which becomes smaller as the spatial headway is shorter.

It is noted that Helbing and Treiber [7] have suggested a constitutive relation for c_0^2

$$c_0^2 = [A_0 + A_1 \tanh(\rho^*)]u^2$$

here, $\rho^*=(\rho-\rho_1)/\Delta\rho$, $\rho_1=0.28\rho_m$, $\Delta\rho=0.1\rho_m$, $A_0=0.008$ and $A_1=0.015$. For the case of $\rho\to 0$ and the previously used values of A_0, A_1, it is easy to find that c_0^2 is negative when ρ^* is close -2.8. This suggests that it would be better to use a value of A_0 larger than A_1 in order to guarantee a positive anticipation coefficient c_0^2. It is also surprisingly noted that in the work of Zhang [24], the sound speed is suggested to be

$$c_0 = \rho du_e/d\rho$$

here, $u_e=q_e/\rho$. Explicitly, the sound speed is again negative for the case of $du_e/d\rho<0$. The problem of whether the expression for traffic sound speed is reasonable can be ascertained by observing if the critical values for traffic regime transition are consistent with the reality.

Considering that based on the physical meaning of c_0, the sound speed in traffic flows should be dependent on the traffic operational condition, we incline to suppose

$$c_0 \propto v_f \tag{10}$$

If the pressure in a traffic jam is identical to the total pressure at the point of flow saturation, using the triangular-form flow–density relation and the quasi-equilibrium approximation denoted by $q\approx q_e$, we can simply yield

$$c_0^2 = \frac{\rho_c/\rho_m}{2(1-\rho_c/\rho_m)}v_f^2 \tag{11}$$

The involved parameters are the saturation and jam densities, both of which depend on the condition of traffic road operation.

Using the definition of traffic flow rate $q=\rho u$ and the expression of vehicular mass conservation $\rho_t+q_x=0$ held under the assumption (i), we can represent B_2 in expression (5) as follows:

$$\left.\begin{aligned}\rho B_2 &= \rho B_{1t} + \rho u B_{1x} - \rho B_1^2 \\ &= 2\rho(u_t + uu_x)_x - 6\rho u_x^2\end{aligned}\right\} \tag{12}$$

indicating that we have

$$T = -p + (\rho v + \mu_1)u_x - \rho\sigma(u_t + uu_x)_x \tag{13}$$

Here, $\mu_1=3\rho\sigma u_x=\rho v_1$. Therefore, considering expressions (7), (9) and (13), and following the principles of mass and momentum conservations, we have the governing equations of the visco-elastic traffic flows

DOI: 10.1002/atr

$$\begin{cases} \rho_t + q_x = 0 \\ \rho(u_t + uu_x) = R \\ R + \left[\rho\sigma(R/\rho)_x\right]_x = -\rho(u-u_e)/\tau - c_0^2\rho_x + \left[\rho(v+v_1)u_x\right]_x \end{cases} \tag{14}$$

The external traffic force $[\rho(u_e - u)/\tau]$ has become more important, and the traffic state equation (8) plays a more significant role in the traffic flow prediction in the visco-elastic traffic flow model. The inclusion of elastic effect allows the traffic flow change with respect to an elastic force, implying that the flow evolution has to make intimately reflection of the influences from operations in both the upstream and downstream neighbourhoods.

For the fixed obstruction problem discussed by Daganzo [8], there is a partition point on the road segment: downstream such point, the traffic flow has a jam density, whereas upstream such point, the traffic density is zero. Therefore, the vehicles on the road segment are fixed without any motion. In the numerical treatment of the fixed obstruction problem, numerical approach plays a key role in determining whether the results are reasonable or not.

The kinematic viscosity of traffic should be proportional to the product of the relaxation time and the anticipation coefficient, that is $v \propto c_0^2\tau$. Hence, the elasticity σ can be calculated by $\sigma \propto l_0^2$; here, $l(=\tau c_0)$ is a characteristic length scale in traffic flows. It is noted that the concern of Daganzo [8] in the application of high-order models, such as the so-called back diffusion of vehicles can be avoided by defining a properly averaged dynamic diffusivity (μ) on the grid interface. For instance, the dynamic diffusivity on the grid interface is defined as $[\mu_{i-1/2} = 2\mu_{i-1}\mu_i/(\mu_{i-1} + \mu_i)]$. The proposed visco-elastic model reduces to a Navier–Stokes type as reported by Kerner and Konhauser [25] if the elasticity vanishes.

Some high-order models involve the replacement of the pressure gradient term in the momentum equation with a velocity gradient term [13,15]. If we can deal with the pressure gradient term carefully in traffic flow simulation, the improper traffic flow density variation for the fixed obstruction problem discussed by Daganzo [8] should not occur.

It is noted that the ramp effect is ignored in the present study. With consideration of the ramp flow effect, the mass conservation equation in Equation (14) should have a source term on the right-hand side, and then, the momentum conservation equation used for describing the vehicular acceleration must be changed accordingly. The traffic state equation (8) is chosen on the basis of the previous work of Del Castillo [22] who proposed a model for the evolution of speed perturbations in dense traffic flows. Another reason of selecting the simpler flow–density relation is that it can provide monotonic values for q'_e in both light and dense traffic flows. This allows us to evaluate the second critical points in traffic flow more conveniently. Evidently, other general forms, such as the Greenshield's model, Greenberg's model [31] and so on, can also be applied in the visco-elastic model, depending on the demand of traffic flow predictions.

It is seen that the viscous diffusion term in Equation (14) includes the effect of v_1, which is determined by the product of the elasticity and the traffic speed gradient. With the assumption of negligible visco-elastic effect, the present model can be reduced to the Euler type model, for which Kiselev *et al.* [32] has presented detailed analysis to include the propagation speed of traffic shock waves and the derivation of the state relationship. They derived the explicit propagation speed of traffic shock waves and found that the saturation density for Greenberg's model is well consistent with the existing data.

The primary reason for further developing the visco-elastic model is that the second-order models include the relaxation time to represent the traffic external force while the elastic effect is not included. In fact, time relaxing is a behaviour in mechanics, and it represents an elastic role in the relevant process. It is a fact that the traffic speed and flow fluctuations in the reality around the equilibrium states also reflect the elastic phenomenon.

3. LINEAR STABILITY ANALYSIS

The values of v, τ and σ could be density dependent, but for the convenience of stability analysis, we assume that they are constant parameters. The linear stability analysis is presented by using the linear

DOI: 10.1002/atr

stability theory of Chandrasekhar [33]. We express the variables with their exponential type disturbances as

$$\begin{cases} \rho = \rho_0 + \tilde{\rho}\exp(\omega t + ikx) \\ u = u_0 + \tilde{u}\exp(\omega t + ikx) \\ q = q_0 + \tilde{q}\exp(\omega t + ikx) \end{cases} \tag{15}$$

The subscript '0' refers to the base state of traffic flow, with the magnitude of the traffic flow rate disturbance given by the supplementary expression $\tilde{q} = u_0\tilde{\rho} + \rho_0\tilde{u}$, and

$$q_e(\rho) = q_e(\rho_0) + q'_e(\rho_0)\tilde{\rho} \tag{16}$$

where $q_e(\rho_0)$=q_0=$\rho_0 u_0$. As detailed in APPENDIX B, we can derive the dispersion relation as

$$\omega^2 + (C + i2ku_0)\omega + ik\left[Cu_0 + C_{1R} + i\left(C_{1I} + ku_0^2\right)\right] = 0 \tag{17}$$

where $q'_e = dq_e/d\rho$, and

$$\begin{cases} C = (\tau^{-1} + vk^2)/(1 - \sigma k^2) \\ C_1 = C_{1R} + iC_{1I} = \left(q'_e - u_0\right)\tau^{-1}/(1 - \sigma k^2) - ikc_0^2/(1 - \sigma k^2) \end{cases} \tag{18}$$

Bearing in mind that the real part of the angular frequency ω should be negative, after some algebraic manipulations, we can express a stability criterion of traffic flows as

$$|J| = \left|\frac{q'_e - u_0}{c_0}\right| \le \left|\frac{1 + v\tau k^2}{\sqrt{1 - \sigma k^2}}\right| \tag{19}$$

When inequality (19) is satisfied, the traffic flow is stable; when the visco-elasticity v=0, σ=0, the result is the same as what was preciously derived by Payne [34]. For the case of non-zero elasticity, it can be concluded that the traffic flow is absolutely unstable as long as the wave number is greater than the critical value 1/σ, suggesting that traffic flow instability occurs for any disturbances with short spatial wavelengths. This is completely consistent with the real traffic flow observations of Kuhne *et al.* [23]. By defining $\sin\theta = k\sqrt{\sigma}$, b_0=$\sigma/(v\tau)$=0.68, it is convenient to find that

$$(\cos\theta)_{\mathrm{cr}} = \left[(0.34|J|)^2 + 1.68\right]^{0.5} - 0.34|J|, \text{for}|J|\ge 1 \tag{20}$$

The critical condition for stable traffic flows becomes

$$k_{\mathrm{cr}} \le k \le 1/\sqrt{\sigma} \tag{21}$$

This means that the traffic flow should be stable for those states whose disturbance wave numbers are in the range given by Equation (21).

With the triangular fundamental diagram shown in Figure 1, the sound speed in a traffic jam c_0 is about 26.11% of the free-flow speed for the operational parameters given in Table 1. The sound speed is about 31.3 km/hour, which is very close the analytical value 35 km/hour, and the experimental data 17.2 miles/hour (=28 km/hour) measured in Lincoln Tunnel in New York, as reported by Kiselev *et al.* [32]. Hence, by according the flow stability criterion given by Equation (19), in the cases of $v \to 0$ and

DOI: 10.1002/atr

Table I. The main parameters of traffic flows on a loop road.

v_f (km/hour)	ρ_c (veh/km/lane)	ρ_m (veh/km/lane)
120	18	150

$\sigma \to 0$, it is convenient for us to find that the critical density for the traffic flow transition from a free-flow regime to a congested oscillating flow regime is equal to the density of saturation (ρ_c). The critical speed for the transition from a congested unstable flow regime to a homogeneously stable regime can be expressed by

$$u_{c2} = c_0 - \left| q'_e \right| \tag{22}$$

It has a value of 14.97 km/hour, with the corresponding second critical density (ρ_{c2}) close to 0.559 ρ_m ($\approx$84 veh/km), at which the average spatial headway of vehicles is about 6 m when the average vehicle length is set as 5.8 m.

4. NUMERICAL VERIFICATION

To verify the present model, numerical test by virtue of a total variation diminishing (TVD) scheme [35] is carried out for congested traffic flows on a loop road with parameters specified in Table 1. The initial traffic speeds, as shown in Figure 2, are assigned in terms of a symmetrical binomial-distribution. The initial densities on the loop road are then evaluated on the basis of the piecewise linear fundamental diagram illustrated in Figure 1. It is noted that the possible maximum magnitude of the initial speed fluctuation is 30 km/hour when the spatially averaged speed denoted by (v_{av}) has values of 72 and 90 km/hour, with the possible maximum magnitude of 10 km/hour corresponding to the cases of v_{av}=15, 16, 20 and c_0 (=31.33) km/hour, respectively.

It is necessary to note that in the solution of Equation (14), the acceleration (R/ρ) and pressure gradient ($c_0^2\rho_x$) are combined to form a new variable (ϕ), which is solved under a periodic condition before the evaluation of density and flow in terms of the TVD. Some detail of the TVD's application can be found elsewhere [4,5].

The parameters for the multiple-case numerical simulation are shown in Table 2. The length scale l_0 is equal to the spatial step Δx. The speed scale is given by $v_0=\rho_c v_f/\rho_m$, with the time scale t_0 calculated by l_0/v_0. Because the density of traffic saturation ρ_c is assigned as 12% of the jam density ρ_m, hence, using the approximation of Equation (11), the ratio of sound speed in a traffic jam to free-flow speed is

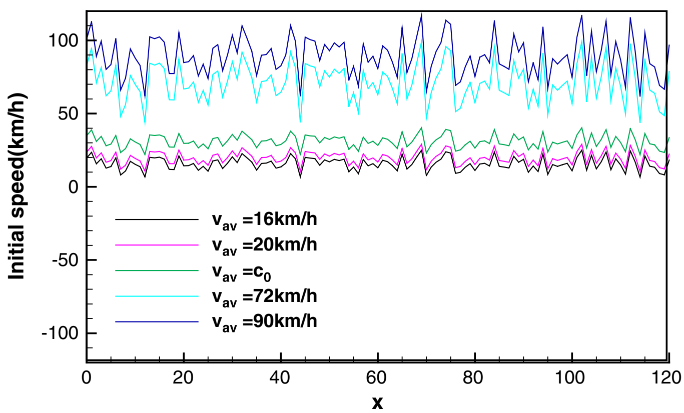

Figure 2. Initial traffic speed on a loop road. It is generated randomly by assuming the speed roughly satisfies a symmetrical binomial-distribution. The used probability density function is PDF(s)=6s(1 − s), $s \in [0,1]$.

DOI: 10.1002/atr

Table II. The parameters for the cases of traffic flow simulation.

Case	$l_0=\Delta x$ (m)	$\mathrm{Re}=(l_0 v_0/\nu)^{a}$	$\hat{\sigma} = 0.68\nu\tau/l_0^2$	v_{av} (km/hour)	$\tau(s)^{b}$
1	160	10	0	90	18.38
2	160	10	3.125×10^{-2}	90	18.38
3	240	10	3.125×10^{-2}	90	27.57
4	320	10	3.125×10^{-2}	90	36.77
5	160	10	3.125×10^{-2}	72	18.38
6	160	10	3.125×10^{-2}	c_0	18.38
7	160	10	3.125×10^{-2}	20	18.38
8	160	10	3.125×10^{-2}	16	18.38
9	160	10	3.125×10^{-2}	15	18.38

[a]The kinematic viscosity is evaluated by $\nu = 0.046c_0^2\tau$, c_0 is given by Equation (11), $v_0=\rho_c v_f/\rho_m=4$m.
[b]The relaxation time is evaluated by $\tau=l_0/c_0$.

about 26.11%. The relaxation time is evaluated as the time taken by an infinitesimal disturbance used to pass through the length l_0, i.e. $\tau=l_0/c_0$. The periodical boundary condition is used in the numerical test of traffic flow simulation.

With the increase of relaxation time, the visco-elastic effect is enhanced, and the distance of speed propagation becomes larger. Therefore, from Figure 3, for $v_{av}=90$km/hour, in the time range of $R_1\in(0,5)$, the instant of speed peak occurrence has delayed. In the time range of $R_2\in(5,10)$, the evolutionary curves of traffic speed have evidently staggered. The valley of the traffic waves is wider in the case of a larger relaxation time. This suggests that, under the same visco-elastic condition, the numerical solutions are rather sensitive to the relaxation time or the spatial step.

A comparison of the visco-elastic traffic model and the purely viscous model can be observed in Figure 4. The evolution of speed is recorded by an observer standing at the station of $x=20$. For the case of an initial mean speed equal to 90km/hour, it is seen that the elastic effect can delay the propagation of traffic speed waves. For example, the delay of the fifth valley arrival can be as large as 6 minutes. The delay effect becomes more evident with increasing time. This indicates that the visco-elastic model can present different traffic flow simulation results as compared with a Navier–Stokes model. To some extent the elastic effect has reflected the interaction between the lead and follower vehicular clusters.

Furthermore, to illustrate the elastic effect, the instantaneous speed–density relation is plotted in Figure 5, in which the observation data extracted from the work of McShane *et al*. [31] are also included and shown by *green* squares. It is seen that there are the hysteresis loops corresponding to the evolutional records of speed and density at $x=20$. In particular, the hysteresis loop becomes narrow at the right end ($\rho>\rho_{c2}\approx0.56$) because of the elastic effect, indicating that the traffic flow speed converges to a value that is slightly larger than the second critical value 15km/hour. On the other hand, the elastic effect on the shape of hysteresis loop alleviates gradually with decreasing density.

From the measured data, it can be estimated that the normalized second critical density is about 0.6, which is quite close to a value of 0.56 obtained on the basis of the sound speed assumption and the

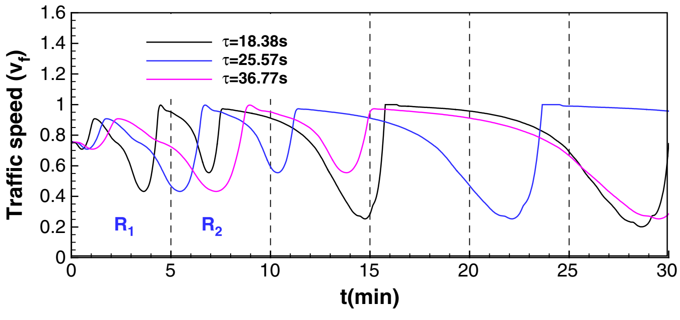

Figure 3. Speed evolution at $x=20$ at different relaxation times for $v_{av}=90$km/hour.

DOI: 10.1002/atr

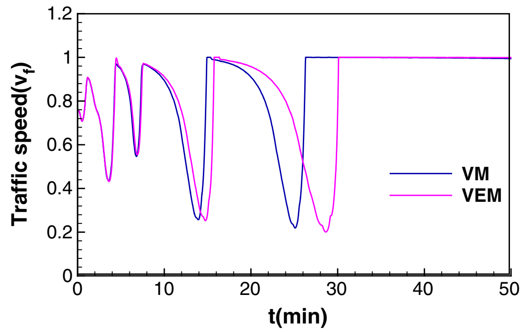

Figure 4. Comparison of the visco-elastic model (VEM) with the pure viscous model (VM) by using the calculated speed evolution at x=20 for v_{av}=90 km/hour.

state equation. The simulated speed–density relations shown in Figure 5(a,b) for the case v_{av}=90 km/hour are in good agreement with the observation results. The instantaneous traffic speed for the special case is close to the observed value, even though the equilibrium flow–density relation is triangular as shown in Figure 1. It suggests that the future inclusion of elastic effects can result in a different speed evolution from that obtained by the VM model, and the difference becomes more evident at the observation section when the density exceeds the second critical density.

The traffic speed evolution at the location of x=20 for the cases of v_{av}=15, 16 and 20 km/hour is shown in Figure 6. In these cases, the traffic flows are highly congested. For the case of v_{av}=20 km/hour, the traffic flow gradually changes into a quasi-steady oscillating regime, and the initial heterogeneity can induce traffic waves propagating to upstream as can be seen in Figure 7(a). The time interval from the speed valley P_1 to another speed valley P_2 is around 78 minutes, whereas the distance of the speed wave propagation is 120 m × 160 m (case 7 in Table 2). Therefore, the reverse

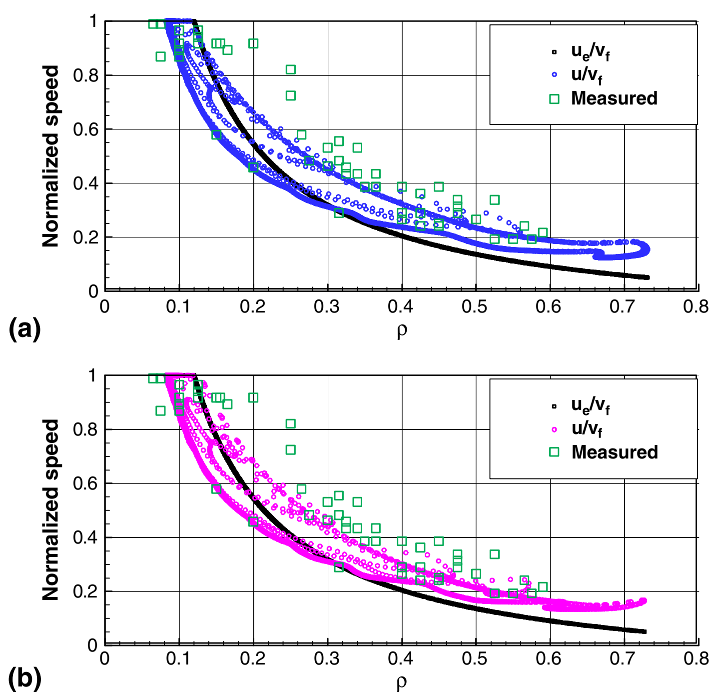

Figure 5. Comparison of the visco-elastic model with the pure viscous model by using the instantaneous speed–density relation at x=20 for v_{av}=90 km/hour. It is noted that the record number is about 12600 in the 10-hour simulation. The observation data are extracted from Ref. [3], and the jam density used in density normalization is assumed to be 200 veh/mile.

DOI: 10.1002/atr

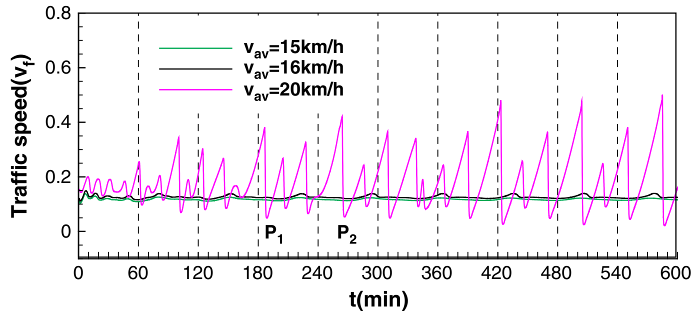

Figure 6. Speed evolution at x=20 under different initial mean speeds.

propagation speed of traffic waves is about 14.8 km/hour. It is noted that this predicted speed is located in the range of 10 to 20 km/hour for the reversely travelling traffic waves, as noted by Helbing and Treiber [7].

However, for the case of v_{av}=16 km/hour, the speed is slightly higher than the second critical speed 14.97 km/hour, corresponding to the second critical density denoted by ρ_{c2} shown in Figure 1, and the initial speed disturbances can be suppressed to some degree by the visco-elastic effect. The weak initial speed waves can be smoothed out, whereas extensive initial speed waves caused by larger gradient can survive. For the case of v_{av}=15 km/hour, the evolutionary curve of traffic speed gradually becomes a horizontal line, implying that the traffic flow has become homogeneous. This is consistent with the result of linear stability analysis. This finding also agrees with the result of Schonhof and Helbing [29] who reported that highly congested traffic flows are homogeneous and stable.

The speed contours in the x–t plane under different conditions can be seen in Figure 7. Part (a) is corresponding to v_{av}=20 km/hour, where the traffic waves travel in the upstream direction. These waves propagate reversely at a speed close to 14.8 km/hour. Part (b) is relevant to v_{av}=90 km/hour, where the traffic speed waves travel to the downstream region. The propagation speed of traffic waves is about 2.7 km/hour.

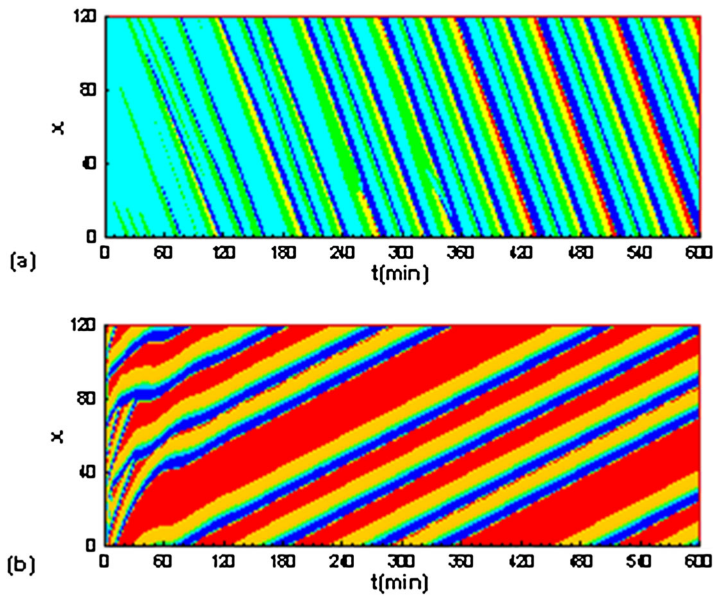

Figure 7. Speed contours in the x–t plane under different initial conditions. (a) v_{av}=20 km/hour, (b) v_{av}=90 km/hour. In part (a), the speed contours are labelled by 0.1, 0.2, 0.3 and 0.4 v_f, whereas in part (b), they are labelled by 0.4, 0.6, 0.7, 0.8 and 0.98 v_f.

DOI: 10.1002/atr

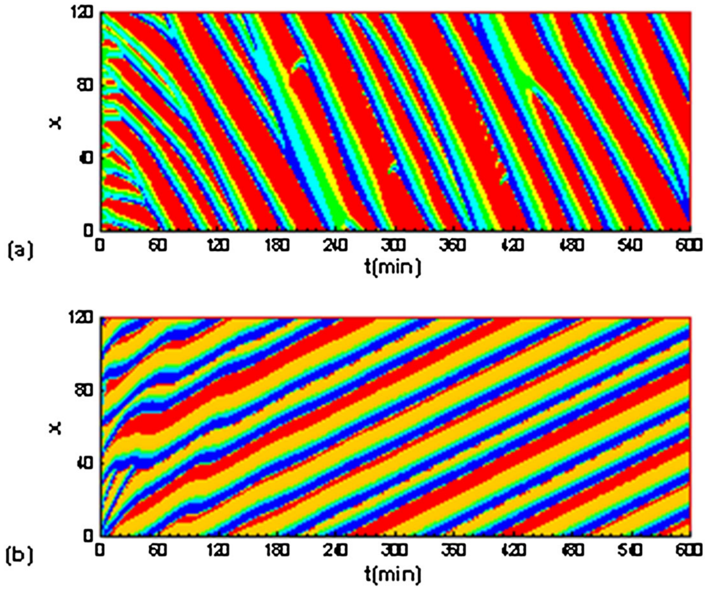

Figure 8. Speed contours in the x–t plane under different initial conditions. (a) $v_{av}=c_0$, (b) v_{av}=72 km/hour. In part (a), the speed contours are labelled by 0.1, 0.2, 0.3 and 0.4 v_f, while in part (b) the speed contours are labelled by 0.4, 0.6, 0.7, 0.8 and 0.98 v_f.

The speed contours in the x–t plane for the cases of $v_{av} = c_0$, and 72 km/hour are shown Figure 8. From part (a), it is seen that the speed of reversely travelling traffic waves is about 7.1 km/hour. On the other hand, from Part (b), it is seen that the speed of forward travelling waves is about 2.9 km/hour. The reason that leads to the difference of wave speed as compared with that related to the cases of Figure 7(a,b) can be attributed to the initial condition, as the relative heterogeneity of initial speed distribution is different as shown in Figure 2.

5. CONCLUSIONS

In summary, the visco-elastic traffic flow model is presented from the constitutive relation for flows of linear visco-elastic fluids. It shows that the viscosity and elasticity are dependent on the traffic sound speed and traffic relaxation time. With a linear stability analysis, it was found that the traffic flow should be absolutely unstable for infinitesimal disturbances with short spatial wavelengths. There are two critical points for the regime transition of traffic flow. First is the numerical calculation of the second critical speed, which is consistent with the critical speed obtained from the theoretical analysis. The second critical point depends on the flow–density relation and the traffic sound speed. If the flow–density relation is in a triangular form, the density of saturation is 12% of the jam density, and the sound speed can be obtained by assuming that the traffic jam pressure is identical to the total pressure at the flow saturation point, the numerical results indicated that the second critical speed is around 15 km/hour at which the flow transition from an oscillating regime to a homogeneously stable regime occurs. For the cases of initial mean speed lower than the second critical speed, the traffic flow is stable, and the initial speed perturbations can be well smoothed out by the visco-elastic effect. For unstable flows, traffic wave propagation manoeuvre is dependent on the initial condition. Because of the inclusion of elastic effect, the present model is more complete than the Navier–Stokes type traffic models.

ACKNOWLEDGEMENTS

This work is supported by National Science Foundation of China (10972212). We are grateful to Dr G.L Chang in University of Maryland and Dr N.N. Smirnov in Moscow State University for some private communications. We also thank the anonymous referees' suggestions.

DOI: 10.1002/atr

APPENDIX A. RELATION BETWEEN $\mathbf{B}_N$ AND $\mathbf{B}_{N+1}$. In Chapter II of Ref.[34], it is easy to find that for $n \geq 1$

$$\mathbf{B}_{n+1}(s) = d\mathbf{B}_n/ds - \mathbf{L}_1\mathbf{B}_n - \mathbf{B}_n\mathbf{L}_1^T \tag{A1}$$

where $\mathbf{L}_1 = \nabla\mathbf{u}$, and $\mathbf{L}_1^T$ is the transpose of tensor $\mathbf{L}_1$. $\mathbf{B}_0 = 1$, and $\mathbf{B}_1 = \mathbf{L}_1 + \mathbf{L}_1^T$.

APPENDIX B. STABILITY ANALYSIS. Some details in the linear stability analysis are given in this appendix. with the perturbations shown in Equation (15), the right-hand term r can be written as

$$\begin{aligned} R = &\left[\frac{q'_e - u_0}{\tau} - \left(kc_0^2\right)i\right]\rho_0\left(\frac{\tilde{\rho}}{\rho_0}\right) \\ &-\rho_0(\tau^{-1} + k^2 v)\tilde{u} + \rho_0\sigma[k^2\omega + k^2(u_0 k)i]\tilde{u} \end{aligned} \tag{B1}$$

whereas the left hand side should be

$$\rho_0[\omega\tilde{u} + i(u_0 k)\tilde{u}] \tag{B2}$$

Therefore, from the second sub-equation in Equation (14), we have

$$C_1\left(\frac{\tilde{\rho}}{\rho_0}\right) + [-C - \omega - (u_0 k)i]\tilde{u} = 0 \tag{B3}$$

with coefficients C and C_1 given by Equation (18).

On the other hand, from the first sub-equation in Equation (14), we can derive

$$[\omega + (u_0 k)i]\left(\frac{\tilde{\rho}}{\rho_0}\right) + ik\tilde{u} = 0 \tag{B4}$$

From the condition that the determinant of the matrix should be vanished

$$\begin{Vmatrix} C_1 & [-C - \omega - (u_0 k)i] \\ [\omega + (u_0 k)i] & ik \end{Vmatrix} = 0 \tag{B5}$$

we can obtain the dispersion relation given by Equation (17). The roots of ω can be expressed as

$$\omega_{1,2} = -\frac{C + i2ku_0}{2} \pm \frac{a + ib}{2} \tag{B6}$$

The real part of $\omega_{1,2}$[=$(-C \pm a)/2$] should not be positive for stable traffic flows.

The coefficients a and b satisfies the following equations:

$$\begin{cases} 2ab = -4kC_{1R} \\ a^2 - b^2 = C + 4kC_{1I} \end{cases} \tag{B7}$$

It means that a^2 can be evaluated from relation

$$a^4 - \left(C^2 + 4kC_{1I}\right)a^2 - 4k^2C_{1R}^2 = 0 \tag{B8}$$

DOI: 10.1002/atr

From the stability criterion of $C^2 \geq a^2$, by some algebraic manipulation, we obtain

$$kC_{1R}^2 \leq -C_{1I}C^2 \tag{B9}$$

Substituting the definitions of C, C_{1R} and C_{1I}, we have the traffic stability criterion

$$|J| = \left|\frac{q'_e - u_0}{c_0}\right| \leq \left|\frac{1 + \nu\tau k^2}{\sqrt{1 - \sigma k^2}}\right| \tag{B10}$$

REFERENCES

1. Lighthill MJ, Whitham GB. On kinematic waves: II. A theory of traffic flow on long crowded roads. *Proceedings of the Royal Society of London. Series A: Mathematical and Physical Sciences* 1955; **229**:317–345.
2. Richards PI. Shock waves on the freeway. *Operations Research* 1956; **4**:42–51.
3. Wong GCK, Wong SC. A multi-class traffic flow model—an extension of LWR model with heterogeneous drivers. *Transportation Research Part A: Policy and Practice* 2002; **36**:827–841.
4. Zhu ZJ, Wu TQ. Two-phase fluids model for freeway traffic and its application to simulate the evolution of solutions in traffic. *ASCE, Journal of Transportation Engineering* 2003; **129**:51–56.
5. Chang GL, Zhu ZJ. A macroscopic traffic model for highway work zones: formulations and numerical results. *Journal of Advanced Transportation* 2006; **40**(3):265–287.
6. Payne HJ. Models of freeway traffic and control. *Simulation Council Proceedings* 1971; **1**:51–61.
7. Helbing D, Treiber M. Gas-kinetic-based traffic model explaining observed hysteretic phase transition. *Physical Review Letters* 1998; **81**:3042–3045.
8. Daganzo C. Requiem for second-order fluid approximations of traffic flow. *Transportation Research Part B: Methodological* 1995; **29**:277–286.
9. Jin WL, Zhang HM. The formation and structure of vehicle clusters in the Payne–Whitham traffic flow model. *Transportation Research Part B: Methodological* 2003; **37**(3):207–223.
10. Zhang P, Wong SC. Essence of conservation forms in the travelling wave solutions of higher-order traffic flow models. *Physical Review E* 2006; **74**(2):026109.
11. Ou ZH, Dai SQ, Zhang P, Dong LY. Nonlinear analysis in the Aw–Rascle anticipation model of traffic flow. *SIAM Journal on Applied Mathematics* 2006; **67**(3):605–618.
12. Klar A, Wegener R. Kinetic derivation of macroscopic anticipation models for vehicular traffic. *SIAM Journal on Applied Mathematics* 2000; **60**(5):1749–1766.
13. Aw A, Rascle M. Resurrection of "second order" models of traffic flow. *SIAM Journal on Applied Mathematics* 2000; **60**:916–938.
14. Kiselev AB, Kokoreva AV, Nikitin VF, Smirnov NN. Mathematical modelling of traffic flow on controlled roads. *Journal of Applied Mathematics and Mechanics* 2004; **68**:933–939.
15. Lebacque JP, Mammar S, Haj-Salem H. The Aw–Rascle and Zhang's model: vacuum problems, existence and regularity of the solutions of Riemann problem. *Transportation Research Part B: Methodological* 2007; **41**(7): 710–721.
16. Zhang P, Wong SC, Dai SQ. A conserved higher order aniso-tropic traffic flow model: Description of equilibrium and non-equilibrium flows. *Transportation Research Part B: Methodological* 2009; **43**(5):562–574.
17. Nagel K, Schreckenberg M. A cellular automaton model for freeway traffic. *Journal de Physique I* 1992; **2**(12): 2221–2229.
18. Helbing D, Huberman BA. Coherent moving states in highway traffic. *Nature* 1998; **396**(6713):738–740.
19. Chowdhury D, Santen L, Schadsschneider A. Statistical physics of vehicular traffic and some related systems. *Physics Reports* 2000; **329**:199–329.
20. Nagatani T. The physics of traffic jams. *Reports on Progress in Physics* 2002; **65**:1331–1386.
21. Helbing D. Traffic and related self-driven many-particle systems. *Reviews of Modern Physics* 2001; **73**:1067–1141.
22. Del Castillo JM. Propagation of perturbations in dense traffic flow: a model and its implications. *Transportation Research Part B: Methodological* 2001; **35**:367–389.
23. Kuhne RD, Michalopoulos P. Continuum flow models. Chapter 5, 2001. Printed at http://www-cta.ornl.gov/cta/research/trb/tft.html.
24. Zhang HM. Driver memory, traffic viscosity and a viscous vehicular traffic flow model. *Transportation Research Part B: Methodological* 2003; **37**:27–41.
25. Kerner BS, Konhauser P. Cluster effect in initially homogeneous traffic flow. *Physical Review E* 1993; **48**: 2335–2338.
26. Hilliges M, Weidlich W. A phenomenological model for dynamic traffic flow in networks. *Transportation Research Part B: Methodological* 1995; **29**(6):407–431.

DOI: 10.1002/atr

27. Han SF. Constitutive Equation and Computational Analytical Theory of Non-Newtonian Fluids. Science Press: Beijing, 2000 (in Chinese).
28. Kerner BS. Synchronized flow as a new traffic phase and related problems for traffic flow modeling. *Mathematical and Computer Modelling* 2002; **35**:481–508.
29. Schonhof M, Helbing D. Criticism of three-phase traffic theory. *Transportation Research Part B: Methodological* 2009; **43**:784–797.
30. Wagner MH. Constitutive analysis of uniaxial elongational flow data of a low-density polyethylene melt. *Journal of Non-Newtonian Fluid Mechanics* 1978; **4**(1–2):39–55.
31. McShane WR, Roess RP, Prassas ES. Traffic Engineering, Chap. 12, 2nd edn. Prentice-Hall: New Jersey, 1998; 282–306.
32. Kiselev AB, Nikitin VF, Smirnov NN, Yumashev MV. Irregular traffic flow on a ring road. *Journal of Applied Mathematics and Mechanics* 2000; **64**(4):627–634.
33. Chandrasekhar S. Hydrodynamic and Hydromagnetic Stability. Oxford University Press: Cambridge, 1961.
34. Payne HJ. FREFLO: a macroscopic simulation model of freeway traffic. *Transportation Research Record* 1979; **722**:68–77.
35. Roe PC. Approximate Riemann solver, parameter vectors, and difference schemes. *Journal of Computational Physics* 1981; **43**:357–372.